

Temporal Dynamics of Normalization Reweighting

Daniel H. Baker, Daniela Marinova, Richard Aveyard, Lydia J. Hargreaves, Alice Renton,
Ruby Castellani, Phoebe Hall, Miriam Harmens, Georgia Holroyd, Beth Nicholson,
Emily L. Williams, Hannah M. Hobson & Alex R. Wade

Department of Psychology, University of York, UK

1 Abstract

For decades, neural suppression in early visual cortex has been thought to be fixed. But recent work has challenged this assumption by showing that suppression can be *reweighted* based on recent history; when pairs of stimuli are repeatedly presented together, suppression between them strengthens. Here we investigate the temporal dynamics of this process using a steady-state visual evoked potential (SSVEP) paradigm that provides a time-resolved, direct index of suppression between pairs of stimuli flickering at different frequencies (5 and 7Hz). Our initial analysis of an existing EEG dataset (N=100) indicated that suppression increases substantially during the first 2-5 seconds of stimulus presentation (with some variation across stimulation frequency). We then collected new EEG data (N=100) replicating this finding for both monocular and dichoptic mask arrangements in a preregistered study designed to measure reweighting. A third experiment (N=20) used source localized MEG, and found that these effects are apparent in primary visual cortex (V1), consistent with results from neurophysiological work. Because long-standing theories propose inhibition/excitation differences in autism, we also compared reweighting between individuals with high vs low autistic traits, and with and without an autism diagnosis, across our 3 data sets (total N=220). We find no compelling differences in reweighting that are associated with autism. Our results support the normalization reweighting model, and indicate that for prolonged stimulation, increases in suppression occur on the order of 2-5 seconds after stimulus onset.

18 2 Introduction

Suppressive interactions between neurons are ubiquitous in the nervous system, with normalization considered a canonical neuronal computation (Carandini & Heeger, 2011). One consequence of normalization is that neurons tuned to different stimulus features modulate each others' firing, usually via a process of divisive suppression (Heeger, 1992). For decades the strength of suppression was treated as fixed, due to the observation that adapting to one stimulus does not decrease its suppressive potency (Foley & Chen, 1997; Freeman et al., 2002). This orthodoxy has been challenged by a series of innovative studies proposing that normalization can be 'reweighted' by recent history (Aschner et al., 2018; Westrick et al., 2016; Yiltiz et al., 2020). When pairs of stimuli are repeatedly presented together, their neural representations appear to suppress each other more strongly. Far from being fixed, normalization may therefore be a dynamic process that is continuously updated by the sensory environment. Our objectives were to measure the timecourse of changes in suppression non-invasively in the human brain, compare them across distinct anatomical pathways, and determine whether they differ as a function of autistic traits.

Plastic changes within the visual system occur over multiple timescales (see Webster, 2015 for a recent review). Cortical forms of adaptation to cues such as stimulus contrast (Blakemore & Campbell, 1969), orientation (Gibson & Radner, 1937) and motion (Mather et al., 2008) can be observed within a few seconds, but also build up over durations on the order of minutes (Greenlee et al., 1991). Other types of adaptation have been identified where changes occur over longer time periods, such as several hours (Kwon et al., 2009) or days (Haak et al., 2014). Previous normalization reweighting studies involved adapting sequences of around 40

– 60s (Aschner et al., 2018; Yiltiz et al., 2020), but in principle reweighting might occur faster than this, consistent with other types of contrast adaptation.

Multiple suppressive pathways have been identified in the visual system, including between stimuli differing in orientation (Foley, 1994; Heeger, 1992), eye-of-origin (Dougherty et al., 2019; Legge, 1979; Sengpiel & Blakemore, 1994) and spatial position (Cannon & Fullenkamp, 1991; Petrov, 2005). At present there is evidence of normalization reweighting between stimuli with orthogonal orientations (Aschner et al., 2018), and adjacent spatial positions (Yiltiz et al., 2020). We anticipated that interocular suppression should also be subject to reweighting, but that there might be differences in the dynamics across suppressive pathways (Li et al., 2005; e.g. Meese & Baker, 2009; Sengpiel & Vorobyov, 2005). Comparing monocular and dichoptic suppression permits any contribution of early pre-cortical factors to be isolated. This is because interocular suppression is generally thought to impact in primary visual cortex (though see Dougherty et al., 2019), and bypasses any retinal and subcortical stages of processing that contribute to monocular suppression (Li et al., 2005).

Atypical sensory experience, including hypersensitivity to loud sounds, bright lights and strong odours or flavours, is widely reported by individuals on the autism spectrum (MacLennan et al., 2022; Simmons et al., 2009), but the causal mechanisms remain unclear. Fundamental measures of sensitivity including visual acuity (Tavassoli et al., 2011), contrast sensitivity (Koh et al., 2010), and audiometric performance (Rosenhall et al., 1999) are not consistently different from neurotypical controls. Theoretical accounts of sensory differences in autism have proposed that the balance of inhibition and excitation may be disrupted (Rosenberg et al., 2015; Rubenstein & Merzenich, 2003), yet the evidence is currently inconclusive (Sandhu et al., 2020; e.g. Schallmo et al., 2020; Van de Cruys et al., 2018). Our recent work identified an autism-related difference using steady-state EEG (Vilidaite et al., 2018), in which nonlinear (second harmonic) responses were weaker, implicating atypical suppression in autism.

Here we perform a time-course analysis of a previously published data set, and report two novel pre-registered experiments using EEG and MEG. Our data show that suppression increases substantially during the first 2–5 seconds following stimulus onset, for both monocular and dichoptic masks. Source localisation of MEG data indicate that the reweighting is present as early as primary visual cortex (V1). We also hypothesised that normalization reweighting might differ as a function of autistic traits, but did not find convincing support for this hypothesis.

3 Materials and Methods

3.1 Participants

Experiment 1 was completed by 100 adult participants (32 male, 68 female; mean age 21.9) in early 2015, and first reported by Vilidaite et al. (2018). Here we reanalysed the dataset, and report the results of masking conditions not previously published. Experiment 2 was completed by 100 adult participants (23 male, 74 female, 3 other/not stated; mean age 22.1) in early 2022. Experiment 3 was completed by 10 adults (2 male, 8 female) with a clinical diagnosis of autism, and 10 control participants who were closely matched for age (means of 21.8 and 22, $t = 0.18$, $df = 18$, $p = 0.86$) and exactly matched for gender. Procedures in Experiments 1 and 2 were approved by the ethics committee of the Department of Psychology at the University of York. Procedures for Experiment 3 were approved by the ethics committee of the York Neuroimaging Centre. All participants provided written informed consent, and procedures were consistent with the Declaration of Helsinki.

3.2 Apparatus and stimuli

In Experiments 1 and 2, stimuli were presented using a ViewPixx 3D LCD display device (VPixx Technologies, Canada) with a resolution of 1920×1080 pixels and a refresh rate of 120Hz. The display was gamma corrected using a Minolta LS110 photometer. In Experiment 2, participants wore active stereo shutter glasses (Nvidia 3D Vision 2) that were synchronised with the display using an infra-red signal. EEG data were collected using a 64-channel Waveguard cap, and were amplified and digitised at 1000Hz using an ANT

84 Neuroscan system. Electrode impedance was maintained below $5\text{k}\Omega$, and referenced to a whole-head average.

85 In Experiment 3, stimuli were presented using a ProPixx DLP projector (VPixx Technologies) running at
86 120Hz. Stereo presentation was enabled using a circular polariser that was synchronised with the projector
87 refresh, and participants wore passive polarised glasses during the experiment. DLP projectors are perfectly
88 linear, so gamma correction was not required. Data were acquired using a refurbished 248-channel 4D
89 Neuroimaging Magnes 3600 MEG scanner, recording at 1001Hz. Participant head shape was digitised using
90 a Polhemus Fastrak device, and head position was recorded at the start and end of each block by passing
91 current through 5 position coils placed at fiducial points on the head. We also obtained structural MRI
92 scans using a 3 Tesla Siemens Magnetom Prisma scanner to aid in source localisation. Two participants were
93 not available for MRI scans, so we used the MNI ICBM152 template brain (Fonov et al., 2011) for these
94 individuals.

95 Stimuli were patches of sine wave grating with a diameter of 2 degrees, flickering sinusoidally (on/off flicker) at
96 either 5Hz or 7Hz. In Experiment 1 the gratings had a spatial frequency of 0.5c/deg, and in Experiments 2 &
97 3 this was increased to 2c/deg. A symmetrical array of 36 individual patches tiled the display. In Experiment
98 1 the patch orientation was randomly selected on each trial, and all patches had the same orientation. In
99 Experiments 2 & 3 each patch had a random orientation, which was intended to prevent any sequential effects
100 between trials with similar orientations. The central patch was omitted and replaced by a fixation marker
101 constructed from randomly overlaid squares. During each experiment, the fixation marker could be resampled
102 on each trial with a probability of 0.5. Participants were instructed to monitor the fixation marker and count
103 the number of times it changed throughout the experiment. This was intended to maintain attention towards
104 the display and keep participants occupied.

105 Participants also completed either the short AQ (Hoekstra et al., 2011) in Experiment 1, or the full AQ
106 (Baron-Cohen et al., 2001) in Experiments 2 and 3. For comparison across experiments, we rescaled the short
107 AQ to the same range as the full AQ (0-50). In Experiments 2 and 3, the sensory perception quotient (SPQ)
108 questionnaire (Tavassoli et al., 2014) was also completed.

109 3.3 Experimental design and statistical analysis

110 In Experiment 1, target stimuli flickering at 7Hz were presented at a range of contrasts (1 - 64%). In half of
111 the conditions a superimposed orthogonal mask of 32% contrast was presented simultaneously, flickering at
112 5Hz. Stimuli were displayed for trials of 11 seconds, with a 3 second inter-trial interval. The experiment
113 consisted of 4 blocks of trials, each lasting around 10 minutes, and resulting in 8 repetitions of each condition.
114 Participants viewed the display from 57cm, were comfortably seated in an upright position, and were able to
115 rest between blocks. Low latency 8-bit digital triggers transmitted the trial onset and condition information
116 directly to the EEG amplifier.

117 The procedure for Experiment 2 was very similar, except that participants also wore stereo shutter glasses
118 during the experiment. There were four conditions: (i) monocular presentation of a 5Hz stimulus of 48%
119 contrast, (ii) monocular presentation of a 7Hz stimulus of 48% contrast, (iii) monocular presentation of both
120 stimuli superimposed at right angles, and (iv) dichoptic presentation of both stimuli at right angles (i.e. one
121 stimulus to the left eye, one to the right eye). Eye of presentation was pseudo-randomised to ensure equal
122 numbers of left-eye and right-eye presentations. The trial duration was 6 seconds, with a 3 second inter-trial
123 interval. Participants completed 3 blocks, each lasting around 10 minutes, resulting in a total of 48 repetitions
124 of each condition. Experiment 3 was identical, except that the projector screen was viewed from a distance of
125 85cm.

126 EEG data from Experiments 1 and 2 were first imported into Matlab using components of the EEGLab
127 toolbox (Delorme & Makeig, 2004), and converted into a compressed ASCII format. Primary data analysis
128 was then conducted using a bespoke R script. In brief, we epoched each trial and extracted the average
129 timecourse across four occipital electrodes (Oz , POz , $O1$ and $O2$), and then calculated the Fourier transform
130 of this average waveform. We excluded trials for which the Mahalanobis distance of the complex Fourier
131 components exceeded 3 (for details see Baker, 2021). This resulted in 0.25% of trials being excluded for
132 Experiment 1, and 4.51% of trials for Experiment 2. Next we averaged the waveforms across all remaining
133 trials, and calculated the Fourier transform in a 1-second sliding window to generate timecourses for each

134 participant. We divided the timecourse for the target-only condition by the timecourse for the target + mask
135 condition to produce a suppression ratio. These were then converted to logarithmic (dB) units for averaging,
136 calculation of standard errors, and statistical comparisons. For display purposes we smoothed the timecourses
137 using a cubic spline function, however all statistical comparisons used the unsmoothed data.

138 Following the suggestion of a reviewer, we conducted an alternative fixed-phase analysis, where the signal
139 in each 1 second epoch was multiplied by a sine wave of appropriate frequency and phase instead of taking
140 the Fourier transform. The results were similar to our main analysis, and can be viewed in the Figures
141 subdirectory of the project code repository (<https://github.com/bakerdh/normreweight/tree/main/Figures>
142 files with the suffix 'FP'). We also conducted simulations (also available in the code repository) to confirm
143 that our analysis methods were not distorting the estimates of the suppression timecourse. In brief, although
144 the 1 second sliding time window does blur the signals in time, these effects are largely negated by calculating
145 the suppression ratio because the blur cancels out across the numerator and denominator. Overall these
146 simulations give us confidence in the accuracy of our estimates of suppression dynamics.

147 For Experiment 3, we performed source localisation using a linearly constrained minimum variance (LCMV)
148 beamformer algorithm, implemented in Brainstorm (Tadel et al., 2011). Structural MRI scans were processed
149 using Freesurfer (Dale et al., 1999) to generate a 3D mesh of the head and brain, and we calculated source
150 weights for each block with reference to a 5-minute empty room recording, usually recorded on the day of
151 the experiment. The matrix of source weights for each block was used in a custom Matlab script to extract
152 signals from V1, identified using the probabilistic maps of Wang et al. (2015). These signals were then
153 imported into R for the main analysis, which was consistent with the EEG analysis described above. The
154 outlier rejection procedure excluded 2.47% of trials for Experiment 3.

155 To make comparisons between groups of participants across time, we used a non-parametric cluster correction
156 technique (Maris & Oostenveld, 2007) based on t-tests. Clusters were identified as temporally adjacent
157 observations that were all statistically significant, and a summed t-value was calculated for each cluster.
158 A null distribution was then generated by randomising group membership and recalculating the summed
159 t-value for the largest cluster, and repeating this procedure 1000 times. Clusters were considered significant if
160 they fell outside of the 95% confidence limits of the null distribution. We adapted this approach to test for
161 significantly increasing suppression by conducting one-way t-tests between time points separated by 1000ms,
162 and repeating the cluster correction procedure as described above.

163 3.4 Preregistration, data and code accessibility

164 Following a preliminary analysis of the data from Experiment 1, we preregistered our hypotheses and analysis
165 plan for Experiments 2 and 3 on the Open Science Framework website. The preregistration document,
166 along with raw and processed data, and analysis scripts, are publicly available at the project repository:
167 <https://osf.io/ab3yv/>

168 4 Results

169 We began by reanalysing data from a steady-state visually evoked potential (SSVEP) experiment reported
170 by Vilidaite et al. (2018). Participants viewed arrays of flickering gratings of varying contrasts. In some
171 conditions a single grating orientation was present flickering at 7Hz (the target), whereas in other conditions
172 a high contrast 'mask' was added at right angles to the target gratings, and flickering at 5Hz. The left panel
173 of Figure 1a shows contrast response functions with and without the mask - the presence of the mask reduces
174 the 7Hz response to the target (blue squares are below the black circles; significant main effect of mask
175 contrast, $F(1,99) = 26.52, p < 0.001$). Similarly, the right panel of Figure 1a shows that the 5Hz response to
176 the mask was itself suppressed by the presence of high contrast targets (main effect of target contrast on the
177 mask response, $F(2.92,288.63) = 46.77, p < 0.001$; note that the data from the masking conditions were not
178 reported by Vilidaite et al. (2018)). At both frequencies, responses were localised to the occipital pole (see
179 insets).

180 We then performed a timecourse analysis, in which we analysed each 11-second trial using a sliding 1-second
181 time window. The top panel of Figure 1c shows the response at the target frequency (7Hz) to a single

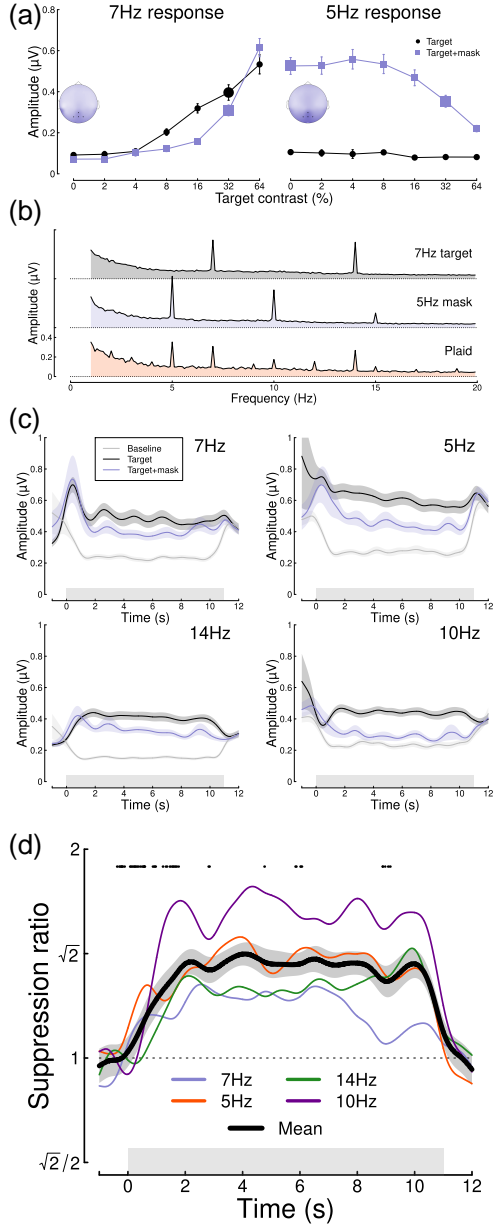


Figure 1: Summary of pilot analysis of data from Vilidiate et al. (2018). Panel (a) shows contrast response functions at the target frequency (7Hz, left) and the mask frequency (5Hz, right). Insets show the distribution of activity across the scalp, with points marking the electrodes over which signals were averaged (Oz, POz, O1 and O2). Panel (b) shows Fourier spectra for the single component stimuli and their combination (plaid). Note the strong second harmonic components at 14Hz and 10Hz. Panel (c) shows timecourses of frequency-locked responses to a single stimulus (black) and the plaid stimulus (blue), compared to a baseline condition (grey) where no stimulus was shown at the target frequency. Panel (d) shows the timecourse of suppression at each frequency (7Hz, 5Hz, 14Hz, 10Hz) and their average (black curve). Points around $y = 1.8$ indicate a significantly increasing ratio (for the time window centred at each point). Error bars in panel (a) and shaded regions in panels (c,d) indicate $\pm 1\text{SE}$ across $N=100$ participants, and grey rectangles indicate the timing of stimulus presentation. The larger symbols in panel (a) indicate the conditions used for subsequent analyses.

182 stimulus of 32% contrast (black), and the response at 7Hz when the 32% contrast mask is added (blue). For
183 comparison, a baseline timecourse is also shown (grey), which was the target response at 7Hz when a 5Hz
184 mask stimulus was shown (therefore controlling for attention, blinking etc.). Analogous responses are shown
185 at three other frequencies - the mask frequency (5Hz), and the second harmonics of both target and mask
186 frequencies (14Hz, 10Hz), at which strong responses were also found (see spectra in Figure 1b). The reduction
187 in signal strength when a second component is added at a different orientation and frequency illustrates
188 the masking effect. Surprisingly there was sometimes substantial activity before and after the stimulus was
189 presented, as is especially clear in the baseline condition shown by the grey curves in Figure 1c. We think the
190 most likely explanation for this is broadband noise from participant movement during the breaks between
191 trials. Since it is approximately equal across conditions it appears to cancel out in the suppression ratios
192 (Figure 1d).

193 Taking the ratio of the two timecourses (the target only timecourse and the target timecourse when a mask
194 was present) to calculate a masking index reveals that for 7Hz targets masking increases steeply during
195 the first two seconds of stimulus presentation, and then plateaus for several seconds (blue trace in Figure
196 1d). A similar pattern is observed for the 5Hz mask (red trace in Figure 1d), as well as at the second
197 harmonics, with some variability in the timecourse across frequencies; for example, at 5Hz suppression peaks
198 at around 4 seconds. The black trace shows the average masking ratio across all four frequencies, which rises
199 steeply for just over two seconds and then stays approximately constant until stimulus offset. We conducted
200 cluster-corrected t-tests between ratios separated by 1000ms, testing for an increase in suppression ratio
201 across time (i.e. a one-sided test). Points at $y = 1.8$ in Figure 1d indicate time points where the ratio is
202 significantly increasing (i.e. there is significantly more suppression 500ms after the time point than there was
203 500ms before it), and occur up until 2.27 seconds after stimulus presentation. We also calculated an overall
204 effect size by comparing the amount of suppression during the first 1000ms following stimulus onset with
205 that between 2000 and 3000ms, averaged across all temporal frequencies. This effect size (Cohen's $d = 0.49$)
206 indicated a medium-sized effect.

207 Our initial reanalysis was promising, however the data were noisy despite the large sample size (of $N=100$),
208 because each participant contributed only 8 trials (88 seconds) to each condition. We therefore preregistered
209 two new experiments (see <https://osf.io/4qudc>) to investigate these effects in greater detail. These had a
210 similar overall design to the Vildaitė et al. (2018) study, with some small changes intended to optimise the
211 study (see Methods). The key differences were that we used shorter trials (because there were few changes
212 in the latter part of the trials shown in Figure 1d), and also focussed all trials into a smaller number of
213 conditions, such that each participant contributed 48 repetitions (288 seconds of data) to each of 4 conditions.

214 Figure 2 summarises the results of our EEG experiment testing a further 100 adult participants. Averaged
215 EEG waveforms showed a strong oscillatory component at each of the two stimulus flicker frequencies (Figure
216 2a), which slightly lagged the driving signal. Signals were well-isolated in the Fourier domain (Figure 2b),
217 and localised to occipital electrodes. Responses at 7Hz were weaker in the two masking conditions, showing
218 significant changes in response amplitude for both the monocular ($t = 7.56, df = 87, p < 0.001$) and dichoptic
219 ($t = 11.35, df = 87, p < 0.001$) masks. Dichoptic masking was significantly stronger than monocular masking
220 ($t = 7.96, df = 87, p < 0.001$), and a similar pattern was evident at 5Hz (note that for this experiment, the
221 terms 'target' and 'mask' are arbitrary, as each component was presented at a single contrast).

222 The timecourse at both flicker frequencies showed an initial onset transient, and was then relatively stable for
223 the 6 seconds of stimulus presentation (Figure 2c,d). The ratio of target only to target + mask conditions
224 increased over time (Figure 2e,f) for both mask types. At 5Hz the increase in masking continued for as
225 long as 5 seconds of stimulus presentation in the monocular condition (Figure 2e; points at $y = 0.8$ indicate
226 significantly increasing suppression, which continue until 5.1s (mon) or 4.2s (dich)), whereas at 7Hz the
227 increase occurred primarily during the first 1.5 seconds after onset (Figure 2f; substantial clusters up to 1.5s
228 (mon) and 1.7s (dich)). These differences across frequency are consistent with the pilot data (see Figure
229 1d). Both monocular and dichoptic masks produced similar timecourses of suppression. We calculated an
230 overall effect size comparing suppression in the first 1000ms after stimulus onset to the time window from
231 3000-4000ms, pooling over frequency and mask type. This had a value of $d = 0.33$. Overall, this second study
232 confirmed that normalization increases during the first few seconds of a steady-state trial, and extends this
233 finding to dichoptic mask arrangements.

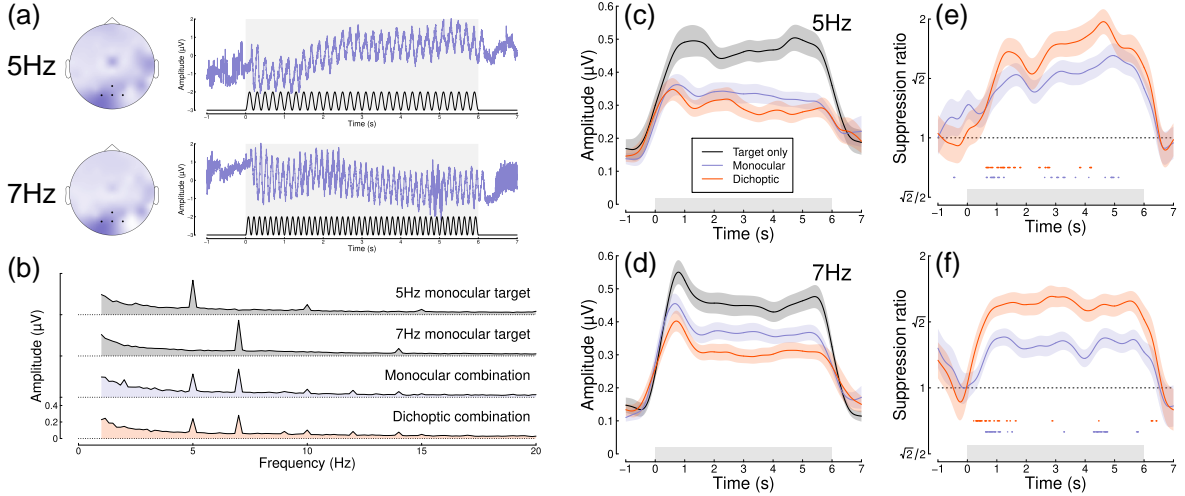


Figure 2: Summary of EEG results for $N=100$ adult participants. Panel (a) shows scalp topographies and averaged waveforms for 5Hz (top) and 7Hz (bottom) stimuli. The black sine wave trace in each panel illustrates the driving contrast modulation, and black points on the scalp topographies indicate electrodes Oz, O1, O2 and POz. Panel (b) shows the Fourier amplitude spectrum for each condition, with clear peaks at 5Hz and 7Hz. Panels (c,d) show timecourses at each frequency for the target-only condition (black), and the monocular (blue) and dichoptic (red) masking conditions. Panels (e,f) show suppression ratios as a function of time for each mask type, with points around $y = 0.8$ indicating a significantly increasing ratio. Shaded regions in panels (c-f) span $\pm 1\text{SE}$ across participants, and light grey rectangles indicate the period of stimulus presentation.

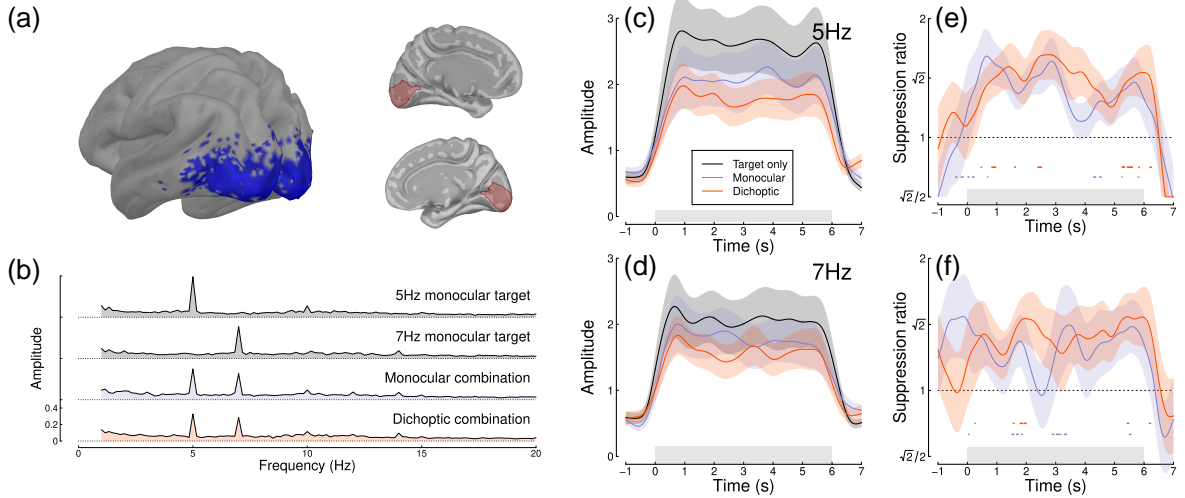


Figure 3: Summary of MEG results for $N=20$ adults. Panel (a) shows average SSVEP response in source space, thresholded at $\text{SNR}=2$ (blue, left), and locations of the V1 ROI on the medial surface of both hemispheres (right, red). Panel (b) shows the Fourier spectra for the four experimental conditions, from the most responsive vertex in V1. Panels (c,d) show timecourses at 5Hz and 7Hz, and panels (e,f) show suppression ratios for the monocular and dichoptic conditions at each frequency, with points around $y = 0.8$ indicating a significantly increasing ratio. Shaded regions in panels (c-f) indicate $\pm 1\text{SE}$ across participants, and light grey rectangles indicate the period of stimulus presentation.

234 Next we repeated the experiment on 20 participants using a 248-channel whole-head cryogenic MEG system.
 235 Half of the participants had a diagnosis of autism, and the remainder were age- and gender-matched controls.
 236 Source localisation using a linearly constrained minimum variance (LCMV) beamformer algorithm (Van Veen
 237 et al., 1997) showed strong localisation of steady-state signals at the occipital pole (see Figure 3a), and in the
 238 Fourier domain (Figure 3b). Responses from the most responsive V1 vertex showed a similar timecourse to
 239 those of the EEG experiments at both frequencies (Figure 3c,d), and showed increasing suppression during
 240 the first few seconds of stimulus presentation (Figure 3e,f). The normalization reweighting effect was again
 241 clearest at 5Hz, especially for the dichoptic condition (red curve in Figure 3e), which increased until 2.5s. This
 242 confirms that the reweighting effects can occur as early as primary visual cortex, consistent with findings from
 243 neurophysiology (Aschner et al., 2018). However the data are more variable than for our EEG experiments,
 244 and had fewer significant clusters, perhaps owing to a power reduction caused by the smaller sample size for
 245 this dataset and greater heterogeneity across frequency. When pooling effects over frequency and condition,
 246 the overall effect size ($d = 0.03$) was near zero.
 247 Intermodulation responses, at sums and differences of different stimulation frequencies, are another marker of
 248 nonlinear interaction (Cunningham et al., 2017; Regan & Regan, 1988; Tsai et al., 2012). We also calculated
 249 the timecourse of the sum intermodulation terms (at 12Hz) in our data sets (the difference terms at 2Hz were
 250 negligible). Figure 4 shows that for both EEG experiments, the intermodulation term increases during the first
 251 1 second of stimulus presentation and then remains approximately constant. The intermodulation response
 252 in the MEG data was less clear, consistent with the spectra shown in Figure 3b. It seems unlikely that
 253 intermodulation terms are useful for monitoring the timecourse of normalization reweighting, and indeed they
 254 may derive from a nonlinear process other than suppression, such as exponentiation and signal combination
 255 (Regan & Regan, 1988). Previous work has identified situations in which suppression is constant, but the
 256 intermodulation term changes substantially between conditions depending on the extent of signal pooling
 257 (Cunningham et al., 2017).

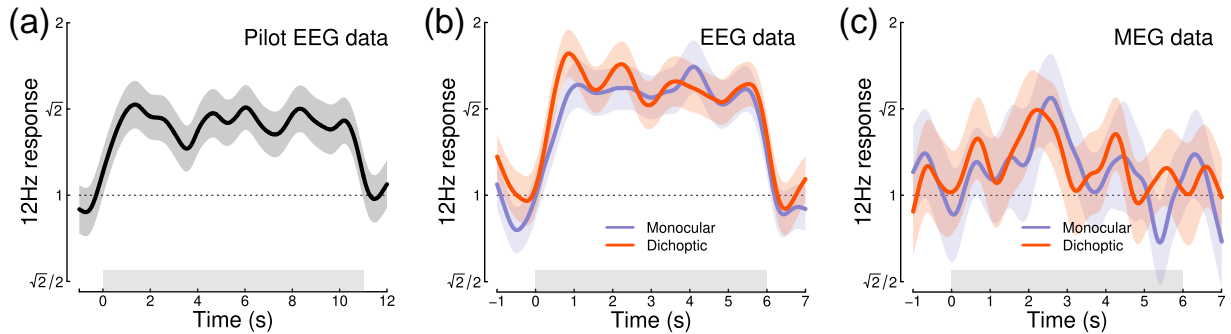


Figure 4: Timecourse of the sum intermodulation term at 12Hz across three experiments. In both EEG experiments, the intermodulation response increases during the first 1 second of stimulus presentation. Responses are calculated as a proportional increase relative to the target-only conditions (where the intermodulation response is absent), for direct comparison with the suppression ratios in Figures 1-3. Shaded regions indicate $\pm 1\text{SE}$.

258 To investigate whether normalization reweighting effects differ with respect to autistic traits, we then split
 259 each dataset (averaged across temporal frequency) using median AQ score (for the EEG experiments) or
 260 according to diagnostic group (autism vs controls) for the MEG data. Figure 5a-c shows distributions of AQ
 261 scores for each experiment, and indicates for the pilot and EEG data which participants were in the high
 262 (purple) and low (green) AQ groups. The median AQ scores were 14 for the pilot data, and 18 for the EEG
 263 data. In the MEG experiment, AQ scores for the autism group (mean 36.1) and the control group (mean
 264 16.7) were significantly different ($t = 6.00, df = 14.2, p < 0.001$), with minimal overlap (one participant with
 265 an autism diagnosis had an AQ score marginally lower than the highest AQ scores from the control group).
 266 These distributions are consistent with previous results for AQ (Baron-Cohen et al., 2001).

267 We compared the timecourse of suppression between groups using a nonparametric cluster correction approach

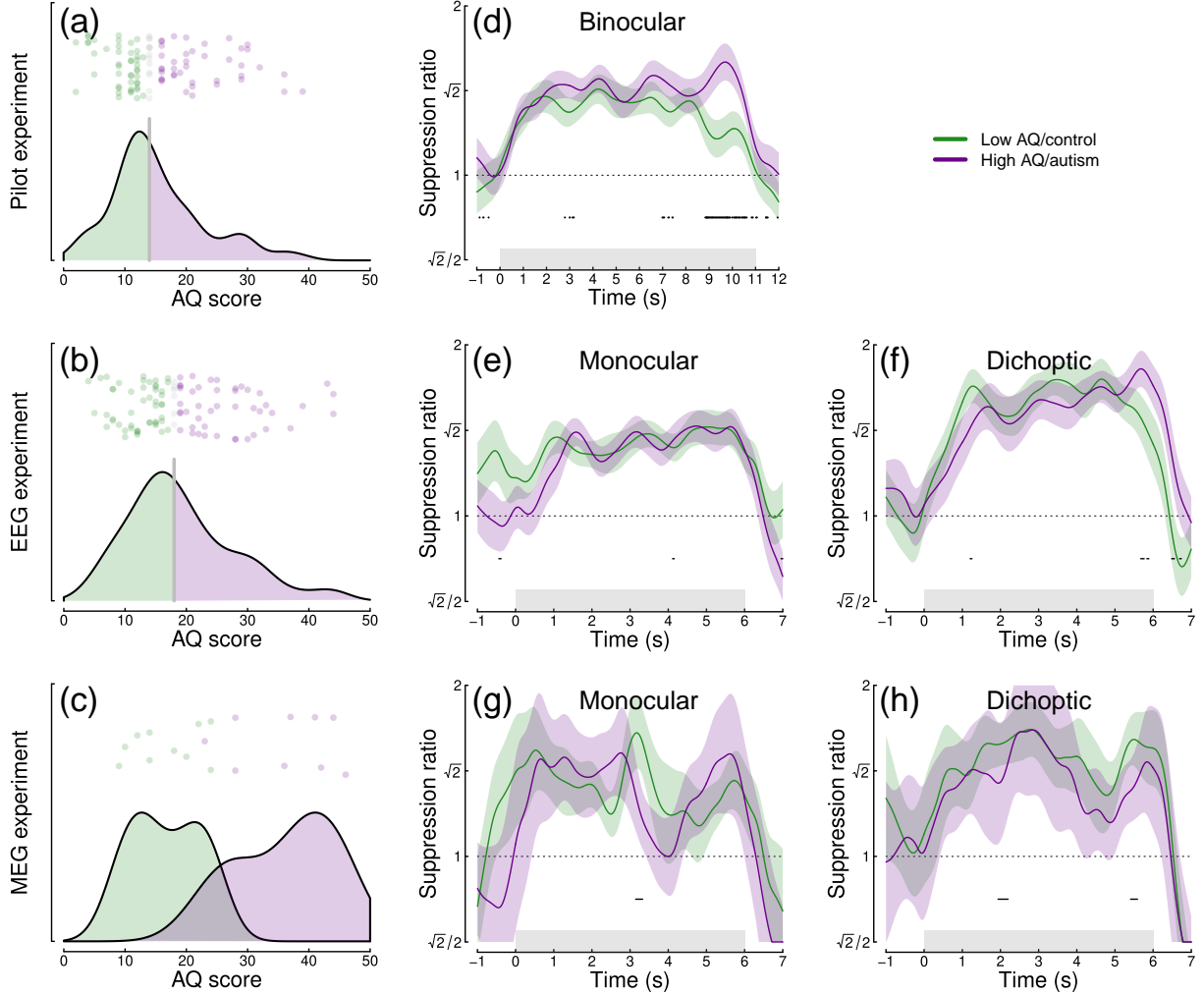


Figure 5: Analysis of the effect of autistic traits on normalization reweighting. Panels (a-c) show distributions of AQ scores across the three data sets. Panels (d-h) show timecourses of suppression averaged across stimulation frequency, and split by AQ score (d-f) or autism status (g, h). Panels (d,e,g) are for binocular or monocular presentation, and panels (f,h) are for dichoptic presentation. Shaded regions in panels (d-h) indicate $\pm 1\text{SE}$ across participants, and black points at $y = 0.8$ indicate significant differences between groups.

268 (Maris & Oostenveld, 2007) to control the type I error rate. Significant clusters are indicated at $y = 0.8$ in
269 panels d-h of Figure 5. Despite some occasionally significant clusters, there is no clear or consistent difference
270 between groups across our three data sets. In particular, none of the significant clusters occur during the first
271 few seconds of stimulus onset, when reweighting takes place. We also compared suppression ratios calculated
272 on Fourier components for the full trial, and found no significant effects of autism on suppression strength.
273 For Experiment 1 we assessed the first and second harmonics separately, but also found no AQ-related
274 differences. We therefore conclude that autism/AQ score is not associated with normalization reweighting, or
275 the strength of suppression more generally.

276 5 Discussion

277 We found evidence of dynamic normalization reweighting across three separate datasets. Suppression increased
278 significantly during the first 2-5 seconds of stimulus presentation, though with some variation across temporal
279 frequency. Relative to the first 1 second of stimulus presentation, the increase in suppression after 3 seconds
280 constituted an effect size of $d = 0.49$ for the pilot data, $d = 0.33$ for our new EEG experiment, and $d =$
281 0.03 for our MEG experiment (pooled across temporal frequency and monocular and dichoptic conditions).
282 Reweighting had a similar timecourse for monocular and dichoptic stimulus presentation, and was apparent as
283 early as V1. We did not find compelling differences associated with autism, or high vs low autistic traits. In
284 the remainder of this section we will discuss possible explanations for temporal frequency differences, evidence
285 for inhibitory differences in autism, and more general implications of dynamic normalization reweighting.

286 One important question is whether the dynamic increase in suppression can be explained by the stimulus onset
287 transient. This is a possibility that cannot be ruled out for some of our data. For example, the steep increase
288 in suppression in Figure 2f has a similar timecourse to the onset transient in Figure 2d. However, there are
289 also counterexamples where suppression continues to increase well beyond the first 1 second of stimulus
290 presentation (e.g. Figure 2e). It is currently unclear why there appear to be such substantial differences
291 between temporal frequency conditions, especially with such similar frequencies (5 and 7Hz). However the
292 differences are relatively consistent across experiments. For example, 5Hz flicker produces a more gradual
293 increase in suppression across all three data sets, compared with 7Hz flicker. These differences may be a
294 consequence of visual channels with different temporal tuning interacting with the stimulation frequency, as
295 well as any nonlinearities that govern suppression. Or there could be an asymmetry, whereby the relative
296 temporal frequency between the two stimulus components affects the character of suppression (Liza & Ray,
297 2022). We hope to be able to model these effects in the future, for example by using dynamic models of early
298 vision that incorporate time-lagged gain control (e.g. Zhou et al., 2019).

299 We did not observe clear differences in the timecourse between monocular and dichoptic suppression. This is
300 important, because the dichoptic arrangement bypasses early stages of processing before the cortex (e.g. the
301 retina and lateral geniculate nucleus). It suggests that the dynamic increases in suppression occur in the
302 cortex, consistent with our MEG data that find evidence of reweighting in V1 (see Fig 3), and with previous
303 neurophysiological work (Aschner et al., 2018). It is currently unclear whether these effects originate in
304 V1, or might involve feedback from higher areas. The similarity between monocular and dichoptic effects
305 also differs from work on adaptation to individual mask components. In both physiological (Li et al., 2005;
306 Sengpiel & Vorobyov, 2005) and psychophysical (Baker et al., 2007) paradigms, adapting to a dichoptic mask
307 reduces its potency, whereas adapting to a monocular mask has little or no effect. Normalization reweighting
308 offers an explanation for why monocular masks presented in isolation do not adapt: if suppressive weights
309 are determined by co-occurrence of stimuli, presentation of an isolated mask will have little effect. However
310 this cannot explain the dichoptic adaptation effects without invoking additional binocular processes, such as
311 competition between summing and differencing channels (e.g. May et al., 2012).

312 The relationship between normalization reweighting and other forms of visual plasticity and adaptation is
313 currently unclear. One phenomenon that might be closely related to our dichoptic effect is the change in
314 interocular suppression that occurs when one eye is patched for a period of time (Lunghi et al., 2011). In
315 the patching paradigm, the inputs to the two eyes are uncorrelated while one eye is patched, which the
316 normalization reweighting model predicts should reduce suppression between the eyes. Most studies using
317 patching have focussed on the resulting imbalance between the patched and non-patched eye, in which the

318 patched eye contributes more to binocular single vision than the non-patched eye. In principle this could be
319 due to increased suppression of the non-patched eye (inconsistent with normalization reweighting), or reduced
320 suppression of the patched eye (consistent with normalization reweighting). It is difficult to distinguish these
321 possibilities using paradigms that assess the balance between the two eyes, such as the binocular rivalry
322 paradigm from the original Lunghi et al. (2011) study. However subsequent work has shown that patching
323 increases the patched eye's response (Zhou et al., 2015), and reduces both dichoptic masking (Baldwin &
324 Hess, 2018) and levels of the inhibitory neurotransmitter GABA (Lunghi et al., 2015). All of these findings
325 are consistent with a reweighting account.

326 Autism is composed of a set of heterogenous symptoms and characteristics, and normalization reweighting
327 may have a more specific relationship to some aspects of autism, rather than autism per se. For this reason,
328 we also examined relationships with the sensory perception quotient (SPQ) to examine whether sensory
329 experiences specifically were related to normalization reweighting. SPQ scores showed significant negative
330 correlation with AQ for the data sets from Experiments 2 and 3 (EEG data, $r = -0.35$, $p < 0.001$; MEG data,
331 $r = -0.57$, $p = 0.011$) with effect sizes comparable to those reported previously (Tavassoli et al., 2014). We also
332 conducted an exploratory analysis of the EEG data from Experiment 2, splitting participants by SPQ instead
333 of AQ. However this analysis did not reveal any convincing differences in normalization reweighting either.
334 Our preregistration also proposed to replicate our earlier finding of a reduced second harmonic response in
335 participants with autism/high AQ scores. However the changes to the experimental design greatly reduced
336 the second harmonic response in both experiments, such that it could not be observed reliably (see Figures
337 2b and 3b). We were therefore not confident in conducting this analysis. We suspect that the increase in
338 spatial frequency from 0.5 c/deg in the Vilidaite et al. (2018) study to 2 c/deg here is most likely responsible
339 for the dramatically reduced second harmonic response.

340 The idea that the dynamic balance of inhibition and excitation might be different in autism (Rosenberg et al.,
341 2015; Rubenstein & Merzenich, 2003) has compelling face validity. For example, individuals with autism often
342 report difficulties with changes in their sensory environment, which might be due to gain control processes
343 failing to adapt appropriately. Indeed, there is experimental evidence of reduced adaptation across various
344 domains (Pellicano et al., 2007; Turi et al., 2015), which is predicted by some autism models (Pellicano &
345 Burr, 2012). However this appears not to extend to changes in normalization reweighting, despite the link
346 between reweighting and adaptation (Westrick et al., 2016).

347 5.1 Conclusions

348 We investigated the timecourse of normalization reweighting across three datasets, with a total of 220
349 participants. We found clear evidence that suppression increases during the first 2-5 seconds of stimulus
350 presentation, though there were differences across frequency that are currently unexplained. We did not
351 find evidence of autism-related differences in either the magnitude or timecourse of suppression. Our results
352 support an emerging theory that suppression is a dynamic process that allows sensory systems to recalibrate
353 according to their recent history.

354 6 Acknowledgements

355 Supported by BBSRC grant BB/V007580/1 awarded to DHB and ARW. We are grateful to all of the
356 participants who took part in the experiments reported here.

357 References

- 358 Aschner, A., Solomon, S. G., Landy, M. S., Heeger, D. J., & Kohn, A. (2018). Temporal contingencies
359 determine whether adaptation strengthens or weakens normalization. *J Neurosci*, 38(47), 10129–10142.
360 <https://doi.org/10.1523/JNEUROSCI.1131-18.2018>
- 361 Baker, D. H. (2021). Statistical analysis of periodic data in neuroscience. *Neurons, Behavior, Data Analysis,
362 and Theory*, 5(3). <https://doi.org/10.51628/001c.27680>
- 363 Baker, D. H., Meese, T. S., & Summers, R. J. (2007). Psychophysical evidence for two routes to suppression

- 364 before binocular summation of signals in human vision. *Neuroscience*, 146(1), 435–448. <https://doi.org/10.1016/j.neuroscience.2007.01.030>
- 365 Baldwin, A. S., & Hess, R. F. (2018). The mechanism of short-term monocular deprivation is not simple:
366 Separate effects on parallel and cross-oriented dichoptic masking. *Sci Rep*, 8(1), 6191. <https://doi.org/10.1038/s41598-018-24584-9>
- 367 Baron-Cohen, S., Wheelwright, S., Skinner, R., Martin, J., & Clubley, E. (2001). The autism-spectrum
368 quotient (AQ): Evidence from asperger syndrome/high-functioning autism, males and females, scientists
369 and mathematicians. *J Autism Dev Disord*, 31(1), 5–17. <https://doi.org/10.1023/a:1005653411471>
- 370 Blakemore, C., & Campbell, F. W. (1969). On the existence of neurones in the human visual system
371 selectively sensitive to the orientation and size of retinal images. *J Physiol*, 203(1), 237–260. <https://doi.org/10.1113/jphysiol.1969.sp008862>
- 372 Cannon, M. W., & Fullenkamp, S. C. (1991). Spatial interactions in apparent contrast: Inhibitory effects
373 among grating patterns of different spatial frequencies, spatial positions and orientations. *Vision Res*,
374 31(11), 1985–1998. [https://doi.org/10.1016/0042-6989\(91\)90193-9](https://doi.org/10.1016/0042-6989(91)90193-9)
- 375 Carandini, M., & Heeger, D. J. (2011). Normalization as a canonical neural computation. *Nature Reviews
376 Neuroscience*, 13(1), 51–62. <https://doi.org/10.1038/nrn3136>
- 377 Cunningham, D. G. M., Baker, D. H., & Peirce, J. W. (2017). Measuring nonlinear signal combination using
378 EEG. *J Vis*, 17(5), 10. <https://doi.org/10.1167/17.5.10>
- 379 Dale, A. M., Fischl, B., & Sereno, M. I. (1999). Cortical surface-based analysis. I. Segmentation and surface
380 reconstruction. *Neuroimage*, 9(2), 179–194. <https://doi.org/10.1006/nim.1998.0395>
- 381 Delorme, A., & Makeig, S. (2004). EEGLAB: An open source toolbox for analysis of single-trial EEG
382 dynamics including independent component analysis. *J Neurosci Methods*, 134(1), 9–21. <https://doi.org/10.1016/j.jneumeth.2003.10.009>
- 383 Dougherty, K., Schmid, M. C., & Maier, A. (2019). Binocular response modulation in the lateral geniculate
384 nucleus. *J Comp Neurol*, 527(3), 522–534. <https://doi.org/10.1002/cne.24417>
- 385 Foley, J. M. (1994). Human luminance pattern-vision mechanisms: Masking experiments require a new model.
386 *J Opt Soc Am A Opt Image Sci Vis*, 11(6), 1710–1719. <https://doi.org/10.1364/josaa.11.001710>
- 387 Foley, J. M., & Chen, C. C. (1997). Analysis of the effect of pattern adaptation on pattern pedestal effects:
388 A two-process model. *Vision Res*, 37(19), 2779–2788. [https://doi.org/10.1016/s0042-6989\(97\)00081-3](https://doi.org/10.1016/s0042-6989(97)00081-3)
- 389 Fonov, V., Evans, A. C., Botteron, K., Almlie, C. R., McKinstry, R. C., Collins, D. L., & Brain Development
390 Cooperative Group. (2011). Unbiased average age-appropriate atlases for pediatric studies. *Neuroimage*,
391 54(1), 313–327. <https://doi.org/10.1016/j.neuroimage.2010.07.033>
- 392 Freeman, T. C. B., Durand, S., Kiper, D. C., & Carandini, M. (2002). Suppression without inhibition in
393 visual cortex. *Neuron*, 35(4), 759–771. [https://doi.org/10.1016/s0896-6273\(02\)00819-x](https://doi.org/10.1016/s0896-6273(02)00819-x)
- 394 Gibson, J. J., & Radner, M. (1937). Adaptation, after-effect and contrast in the perception of tilted lines.
395 I. Quantitative studies. *Journal of Experimental Psychology*, 20(5), 453–467. <https://doi.org/10.1037/h0059826>
- 396 Greenlee, M. W., Georgeson, M. A., Magnussen, S., & Harris, J. P. (1991). The time course of adaptation to
397 spatial contrast. *Vision Res*, 31(2), 223–236. [https://doi.org/10.1016/0042-6989\(91\)90113-j](https://doi.org/10.1016/0042-6989(91)90113-j)
- 398 Haak, K. V., Fast, E., Bao, M., Lee, M., & Engel, S. A. (2014). Four days of visual contrast deprivation reveals
399 limits of neuronal adaptation. *Curr Biol*, 24(21), 2575–2579. <https://doi.org/10.1016/j.cub.2014.09.027>
- 400 Heeger, D. J. (1992). Normalization of cell responses in cat striate cortex. *Vis Neurosci*, 9(2), 181–197.
401 <https://doi.org/10.1017/s0952523800009640>
- 402 Hoekstra, R. A., Vinkhuyzen, A. A. E., Wheelwright, S., Bartels, M., Boomsma, D. I., Baron-Cohen, S.,
403 Posthuma, D., & Sluis, S. van der. (2011). The construction and validation of an abridged version of the
404 autism-spectrum quotient (AQ-short). *J Autism Dev Disord*, 41(5), 589–596. <https://doi.org/10.1007/s10803-010-1073-0>
- 405 Koh, H. C., Milne, E., & Dobkins, K. (2010). Spatial contrast sensitivity in adolescents with autism spectrum
406 disorders. *J Autism Dev Disord*, 40(8), 978–987. <https://doi.org/10.1007/s10803-010-0953-7>
- 407 Kwon, M., Legge, G. E., Fang, F., Cheong, A. M. Y., & He, S. (2009). Adaptive changes in visual cortex
408 following prolonged contrast reduction. *J Vis*, 9(2), 20.1–16. <https://doi.org/10.1167/9.2.20>
- 409 Legge, G. E. (1979). Spatial frequency masking in human vision: Binocular interactions. *J Opt Soc Am*,
410 69(6), 838–847. <https://doi.org/10.1364/josa.69.000838>
- 411 Li, B., Peterson, M. R., Thompson, J. K., Duong, T., & Freeman, R. D. (2005). Cross-orientation suppression:

- 418 Monoptic and dichoptic mechanisms are different. *J Neurophysiol*, 94(2), 1645–1650. <https://doi.org/10.1152/jn.00203.2005>
- 419 Liza, K., & Ray, S. (2022). Local interactions between steady-state visually evoked potentials at nearby
420 flickering frequencies. *J Neurosci*, 42(19), 3965–3974. <https://doi.org/10.1523/JNEUROSCI.0180-22.2022>
- 421 Lunghi, C., Burr, D. C., & Morrone, C. (2011). Brief periods of monocular deprivation disrupt ocular balance
422 in human adult visual cortex. *Curr Biol*, 21(14), R538–9. <https://doi.org/10.1016/j.cub.2011.06.004>
- 423 Lunghi, C., Emir, U. E., Morrone, M. C., & Bridge, H. (2015). Short-term monocular deprivation alters GABA
424 in the adult human visual cortex. *Curr Biol*, 25(11), 1496–1501. <https://doi.org/10.1016/j.cub.2015.04.021>
- 425 MacLennan, K., O'Brien, S., & Tavassoli, T. (2022). In our own words: The complex sensory experiences of
426 autistic adults. *J Autism Dev Disord*, 52(7), 3061–3075. <https://doi.org/10.1007/s10803-021-05186-3>
- 427 Maris, E., & Oostenveld, R. (2007). Nonparametric statistical testing of EEG- and MEG-data. *J Neurosci
428 Methods*, 164(1), 177–190. <https://doi.org/10.1016/j.jneumeth.2007.03.024>
- 429 Mather, G., Pavan, A., Campana, G., & Casco, C. (2008). The motion aftereffect reloaded. *Trends Cogn Sci*,
430 12(12), 481–487. <https://doi.org/10.1016/j.tics.2008.09.002>
- 431 May, K. A., Zhaoping, L., & Hibbard, P. B. (2012). Perceived direction of motion determined by adaptation
432 to static binocular images. *Curr Biol*, 22(1), 28–32. <https://doi.org/10.1016/j.cub.2011.11.025>
- 433 Meese, T. S., & Baker, D. H. (2009). Cross-orientation masking is speed invariant between ocular pathways
434 but speed dependent within them. *Journal of Vision*, 9(5), 2. <https://doi.org/10.1167/9.5.2>
- 435 Pellicano, E., & Burr, D. (2012). When the world becomes 'too real': A bayesian explanation of autistic
436 perception. *Trends Cogn Sci*, 16(10), 504–510. <https://doi.org/10.1016/j.tics.2012.08.009>
- 437 Pellicano, E., Jeffery, L., Burr, D., & Rhodes, G. (2007). Abnormal adaptive face-coding mechanisms in
438 children with autism spectrum disorder. *Curr Biol*, 17(17), 1508–1512. [https://doi.org/10.1016/j.cub.2007.07.065](https://doi.org/10.1016/j.cub.
439 2007.07.065)
- 440 Petrov, Y. (2005). Two distinct mechanisms of suppression in human vision. *Journal of Neuroscience*, 25(38),
441 8704–8707. <https://doi.org/10.1523/jneurosci.2871-05.2005>
- 442 Regan, M. P., & Regan, D. (1988). A frequency domain technique for characterizing nonlinearities in biological
443 systems. *Journal of Theoretical Biology*, 133(3), 293–317. [https://doi.org/https://doi.org/10.1016/S0022-5193\(88\)80323-0](https://doi.org/https://doi.org/10.1016/S0022-
444 5193(88)80323-0)
- 445 Rosenberg, A., Patterson, J. S., & Angelaki, D. E. (2015). A computational perspective on autism. *Proc Natl
446 Acad Sci U S A*, 112(30), 9158–9165. <https://doi.org/10.1073/pnas.1510583112>
- 447 Rosenhall, U., Nordin, V., Sandström, M., Ahlsén, G., & Gillberg, C. (1999). Autism and hearing loss. *J
448 Autism Dev Disord*, 29(5), 349–357. <https://doi.org/10.1023/a:1023022709710>
- 449 Rubenstein, J. L. R., & Merzenich, M. M. (2003). Model of autism: Increased ratio of excitation/inhibition in
450 key neural systems. *Genes Brain Behav*, 2(5), 255–267. <https://doi.org/10.1034/j.1601-183x.2003.00037.x>
- 451 Sandhu, T. R., Reese, G., & Lawson, R. P. (2020). Preserved low-level visual gain control in autistic adults.
452 *Wellcome Open Research*, 4(208). <https://doi.org/10.12688/wellcomeopenres.15615.1>
- 453 Schallmo, M.-P., Kolodny, T., Kale, A. M., Millin, R., Flevaris, A. V., Edden, R. A. E., Gerdts, J., Bernier,
454 R. A., & Murray, S. O. (2020). Weaker neural suppression in autism. *Nat Commun*, 11(1), 2675.
455 <https://doi.org/10.1038/s41467-020-16495-z>
- 456 Sengpiel, F., & Blakemore, C. (1994). Interocular control of neuronal responsiveness in cat visual cortex.
457 *Nature*, 368(6474), 847–850. <https://doi.org/10.1038/368847a0>
- 458 Sengpiel, F., & Vorobyov, V. (2005). Intracortical origins of interocular suppression in the visual cortex. *J
459 Neurosci*, 25(27), 6394–6400. <https://doi.org/10.1523/JNEUROSCI.0862-05.2005>
- 460 Simmons, D. R., Robertson, A. E., McKay, L. S., Toal, E., McAleer, P., & Pollick, F. E. (2009). Vision in autism
461 spectrum disorders. *Vision Research*, 49(22), 2705–2739. <https://doi.org/10.1016/j.visres.2009.08.005>
- 462 Tadel, F., Baillet, S., Mosher, J. C., Pantazis, D., & Leahy, R. M. (2011). Brainstorm: A user-friendly
463 application for MEG/EEG analysis. *Comput Intell Neurosci*, 2011, 879716. [https://doi.org/10.1155/2011/879716](https://doi.org/10.1155/
464 2011/879716)
- 465 Tavassoli, T., Hoekstra, R. A., & Baron-Cohen, S. (2014). The sensory perception quotient (SPQ): Develop-
466 ment and validation of a new sensory questionnaire for adults with and without autism. *Mol Autism*, 5,
467 29. <https://doi.org/10.1186/2040-2392-5-29>
- 468 Tavassoli, T., Latham, K., Bach, M., Dakin, S. C., & Baron-Cohen, S. (2011). Psychophysical measures of
469 visual acuity in autism spectrum conditions. *Vision Research*, 51(15), 1778–1780. [https://doi.org/10.1016/j.visres.2011.06.004](https://doi.org/10.
470 1016/j.visres.2011.06.004)

- 472 Tsai, J. J., Wade, A. R., & Norcia, A. M. (2012). Dynamics of normalization underlying masking in human
473 visual cortex. *J Neurosci*, 32(8), 2783–2789. <https://doi.org/10.1523/JNEUROSCI.4485-11.2012>
- 474 Turi, M., Burr, D. C., Igliozi, R., Aagten-Murphy, D., Muratori, F., & Pellicano, E. (2015). Children with
475 autism spectrum disorder show reduced adaptation to number. *Proc Natl Acad Sci U S A*, 112(25),
476 7868–7872. <https://doi.org/10.1073/pnas.1504099112>
- 477 Van de Cruys, S., Vanmarcke, S., Steyaert, J., & Wagemans, J. (2018). Intact perceptual bias in autism
478 contradicts the decreased normalization model. *Scientific Reports*, 8(1). <https://doi.org/10.1038/s41598-018-31042-z>
- 480 Van Veen, B. D., Drongelen, W. van, Yuchtman, M., & Suzuki, A. (1997). Localization of brain electrical
481 activity via linearly constrained minimum variance spatial filtering. *IEEE Trans Biomed Eng*, 44(9),
482 867–880. <https://doi.org/10.1109/10.623056>
- 483 Vilidaite, G., Norcia, A. M., West, R. J. H., Elliott, C. J. H., Pei, F., Wade, A. R., & Baker, D. H. (2018).
484 Autism sensory dysfunction in an evolutionarily conserved system. *Proc Biol Sci*, 285(1893), 20182255.
485 <https://doi.org/10.1098/rspb.2018.2255>
- 486 Wang, L., Mruczek, R. E. B., Arcaro, M. J., & Kastner, S. (2015). Probabilistic maps of visual topography
487 in human cortex. *Cereb Cortex*, 25(10), 3911–3931. <https://doi.org/10.1093/cercor/bhu277>
- 488 Webster, M. A. (2015). Visual adaptation. *Annu Rev Vis Sci*, 1, 547–567. <https://doi.org/10.1146/annurev-vision-082114-035509>
- 489 Westrick, Z. M., Heeger, D. J., & Landy, M. S. (2016). Pattern adaptation and normalization reweighting.
490 *Journal of Neuroscience*, 36(38), 9805–9816. <https://doi.org/10.1523/jneurosci.1067-16.2016>
- 491 Yiltiz, H., Heeger, D. J., & Landy, M. S. (2020). Contingent adaptation in masking and surround suppression.
492 *Vision Res*, 166, 72–80. <https://doi.org/10.1016/j.visres.2019.11.004>
- 493 Zhou, J., Baker, D. H., Simard, M., Saint-Amour, D., & Hess, R. F. (2015). Short-term monocular
494 patching boosts the patched eye's response in visual cortex. *Restor Neurol Neurosci*, 33(3), 381–387.
495 <https://doi.org/10.3233/RNN-140472>
- 496 Zhou, J., Benson, N. C., Kay, K., & Winawer, J. (2019). Predicting neuronal dynamics with a delayed gain
497 control model. *PLoS Comput Biol*, 15(11), e1007484. <https://doi.org/10.1371/journal.pcbi.1007484>